L-arginine-Functionalized Pillar[5]arene-based Supramolecular Photosensitizer for Synergistically Enhanced Cancer Therapeutic Effectiveness

Shuang Chao,‡[ab] Ziyan Shen,‡[a] Bowen Li,[a] Yuxin Pei,[a] and Zhichao Pei*[ab]

[a]*Shaanxi Key Laboratory of Natural Products & Chemical Biology, College of Chemistry & Pharmacy, Northwest A&F University, Yangling 712100, P. R. China. E-mail: peizc@nwafu.edu.cn; Fax: +86-29-8709-2769; Tel: +86-29-8709-2769*
[b]*College of Plant protection, Northwest A&F University, Yangling, Shaanxi, 712100, China.*
‡ These authors contributed equally.

Supporting Information

1. General information

All reagents were purchased from commercial suppliers and used without further purification unless specified. Water used in this work was triple distilled. ^{1}H NMR spectra were recorded on a Bruker 500 MHz Spectrometer, with working frequencies of 500 MHz for ^{1}H and 125 MHz for ^{13}C nuclei, respectively. SEM image was obtained using a Nano SEM-450 (FEI, U.S.A.) with an accelerating voltage of 10.0 kV. TEM image was obtained by TECNAI G2 SPIRIT BIO (FEI, U.S.A.). DLS measurements were performed on a DelsaTM Nano system (Beckman Coulter, U.S.A.). K_a was measured from Nano-ITC SV (TA-Waters LLC, U.S.A.). UV-vis spectra were recorded with Shimadzu 1750 UV-visible spectrophotometer (Japan) at 298 K. Human liver hepatocellular carcinoma HepG2, and human liver HL7702, were obtained from KeyGEN BioTECH Co. (Nanjing, China). Cell culture was carried out in an incubator with a humidified atmosphere of 5% CO_2 at 37 °C. Dihydrorhodamine 123 (DHR123), Dihydroethidium (DHE), hydroxyphenyl fluorescein (HPF), singlet oxygen sensor green (SOSG) were purchased from MKbio (China). The green fluorescent probes for labeling Endoplasmic reticula, mitochondria, lysosomes, and Golgi apparatuses were purchased from Beyotime (China). Annexin V-EGFP/PI apoptosis detection kit was purchased from Solarbio (China).

2. Live subject statement

All experiments were performed in accordance with the International Ethical Guidelines for Biomedical Research Involving Human Subjects of World Health Organization, and approved by the Northwest A&F University Animal Care Committee.

3. Synthesis and characterizations

The synthesis routes of LAP5 and NBSPD are shown in Scheme S1 and Scheme S2, respectively.

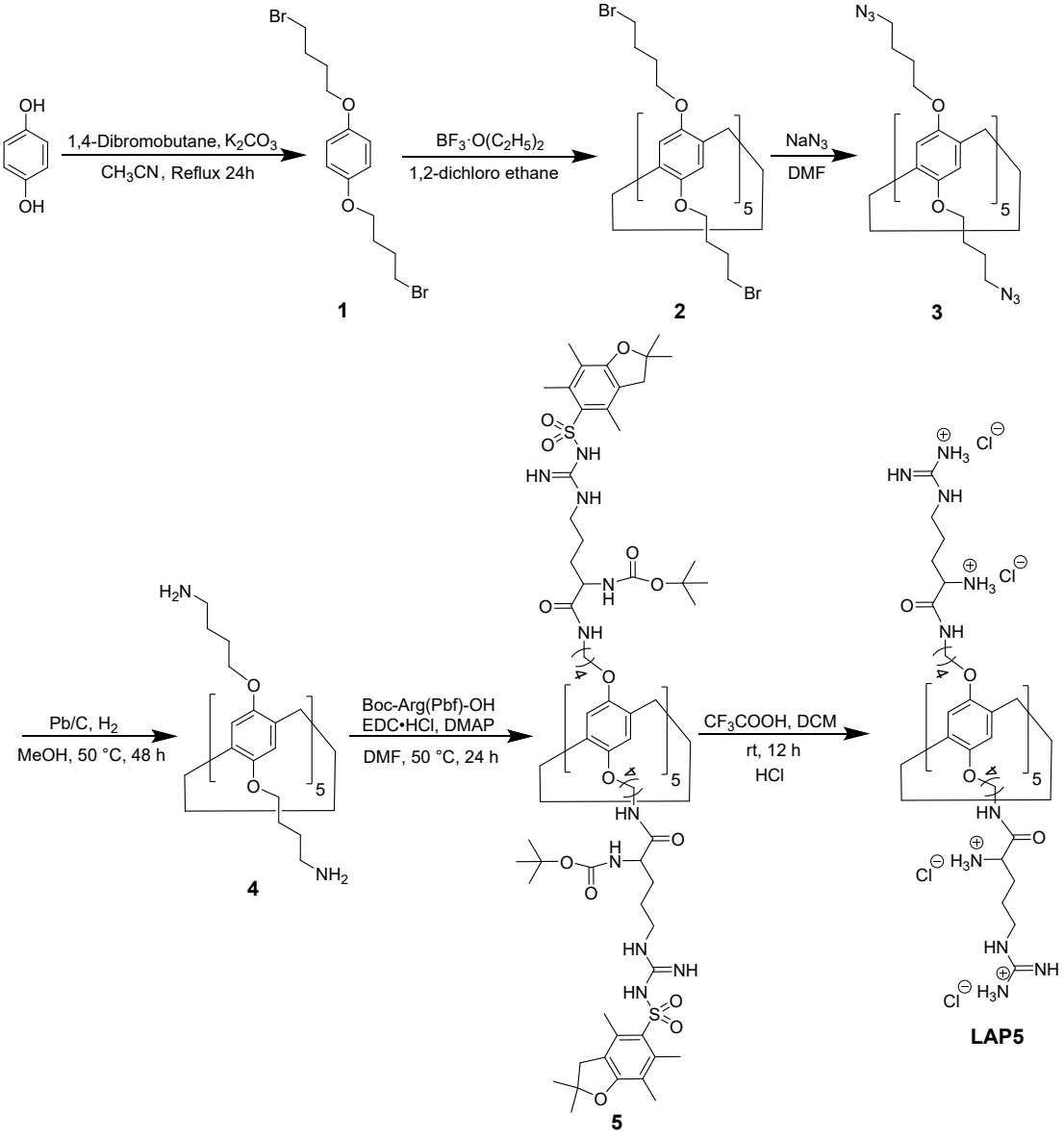

Scheme S1 Synthetic route of LAP5.

Compounds 1, 2, 3, and 4 were synthesized according to our previous method.[1, 2] The ^{1}H NMR spectrum of compound 1 was shown in Fig. S1. ^{1}H NMR (500 MHz, $CDCl_3$) δ (ppm): 6.81 (s, 4 H), 3.94 (t, J = 6.0 Hz, 4 H), 3.48 (t, J = 6.5 Hz, 4 H), 2.09-2.03 (m, 4 H), 1.94-1.88 (m, 4 H). The ^{1}H NMR spectrum of compound 2 was shown in Fig. S2. ^{1}H NMR (500 MHz, $CDCl_3$) δ (ppm): 6.82 (s, 10 H), 3.94 (t, J = 5.0 Hz, 20 H), 3.76 (s, 10 H), 3.45 (t, J = 5.0 Hz, 20 H), 2.08-2.05 (m,

20 H), 1.95-1.93 (m, 20 H). The ^{1}H NMR spectrum of compound 3 was shown in Fig. S3. ^{1}H NMR (500 MHz, $CDCl_3$, 298.15 K) δ (ppm): 6.84 (s, 10 H), 3.92 (t, J = 5.0 Hz, 20 H), 3.76 (s, 10 H), 3.37 (t, J = 5.0 Hz, 20 H), 1.92-1.87 (m, 20 H), 1.86-1.81 (m, 20 H). The ^{1}H NMR spectrum of compound 4 was shown in Fig. S4. ^{1}H NMR (400 MHz, MeOH-d_4, 298.15 K) δ (ppm): 6.83 (s, 10 H), 3.90 (t, J = 8.0 Hz, 20 H), 3.76 (s, 10 H), 2.83 (t, J = 8.0 Hz, 20 H), 1.86-1.84 (m, 20 H), 1.80-1.78 (m, 20 H).

Synthesis of compound 5. A mixture of compound 4 (20 mg, 0.015 mmol), Boc-Arg(Pbf)-OH） (158.76 mg, 0.3 mmol), DMAP (37 mg, 0.3 mmol) and EDC•HCl (57.79 mg, 0.3 mmol) in 5 mL DMF was stirred at 50 ℃ for 24 h, then 20 mL DCM was added into the mixture. The mixture was washed with water (2 × 20 mL), saturated NaCl (2 × 20 mL) and 1 M HCl (2 × 20 mL). The organic phase was dried with $NaSO_4$ and concentrated under reduced pressure. The crude product was purified by flash column chromatography (DCM/CH_3OH, v/v = 20:1) to give compound 5 as a white solid (19.7 mg, 27 %). The ^{1}H NMR and ^{13}C NMR spectrums of compound 5 were shown in Fig. S5-6. ^{1}H NMR (400 MHz, DMSO-d_6, 298.15 K) δ (ppm): 7.88 (s, 10 H), 6.81 (s, 10 H), 6.75 (s, 10 H), 6.66-6.40 (m, 20 H), 4.02 (s, 10 H), 3.88 (s, 10 H), 3.72 (m, 20 H), 3.16 (s, 20 H), 3.03 (s, 20 H), 2.93 (s, 20 H), 2.48 (s, 30 H), 2.43 (s, 30 H), 2.00 (s, 30 H), 1.77-1.85 (m, 50 H), 1.39-1.35 (m, 190 H). ^{13}C NMR (125 MHz, DMSO-d_6, 298.15 K) δ (ppm): 171.86, 157.43, 156.04, 155.23, 148.95, 137.24, 134.17, 131.41, 127.90, 124.22, 116.20, 113.98, 86.17, 78.00, 67.55, 54.80, 54.08, 42.46, 38.36, 29.46, 28.22, 28.09, 26.69, 25.94, 25.67, 18.87, 17.52, 12.18.

Synthesis of compound LAP5. 5 mL CF_3COOH was added drop by drop into a solution of compound 5 (80 mg, 0.016 mmol in 5 mL DCM) in ice-bath. The mixture was stirred at room temperature for 2 h, then concentrated under reduced pressure. The crude product was treated with saturated $NaHCO_3$ solution. The white solid was collected and washed with water for 3 times to give LAP5 (52 mg, 90 %). The ^{1}H NMR and ^{13}C NMR spectrums of compound LAP5 were shown in Fig. S7-8. ^{1}H NMR (400 MHz, D_2O/DMSO-d_6 = 1/1, 298.15 K) δ (ppm): 6.73 (s, 10 H), 3.82 (s, 10 H), 3.69 (s, 10 H), 3.58 (s, 10 H), 3.19 (s, 20 H), 3.06 (s, 20 H), 1.74-1.68 (m, 60 H), 1.50 (s, 20 H). ^{13}C NMR (125 MHz, D_2O/DMSO-d_6 = 1/1, 298.15 K) δ (ppm): 169.83, 157.67, 150.56, 129.72, 116.00, 69.35, 53.64, 41.50, 40.39, 40.33, 30.69, 30.14, 29.28, 27.95, 27.88, 26.81, 26.76, 25.00.

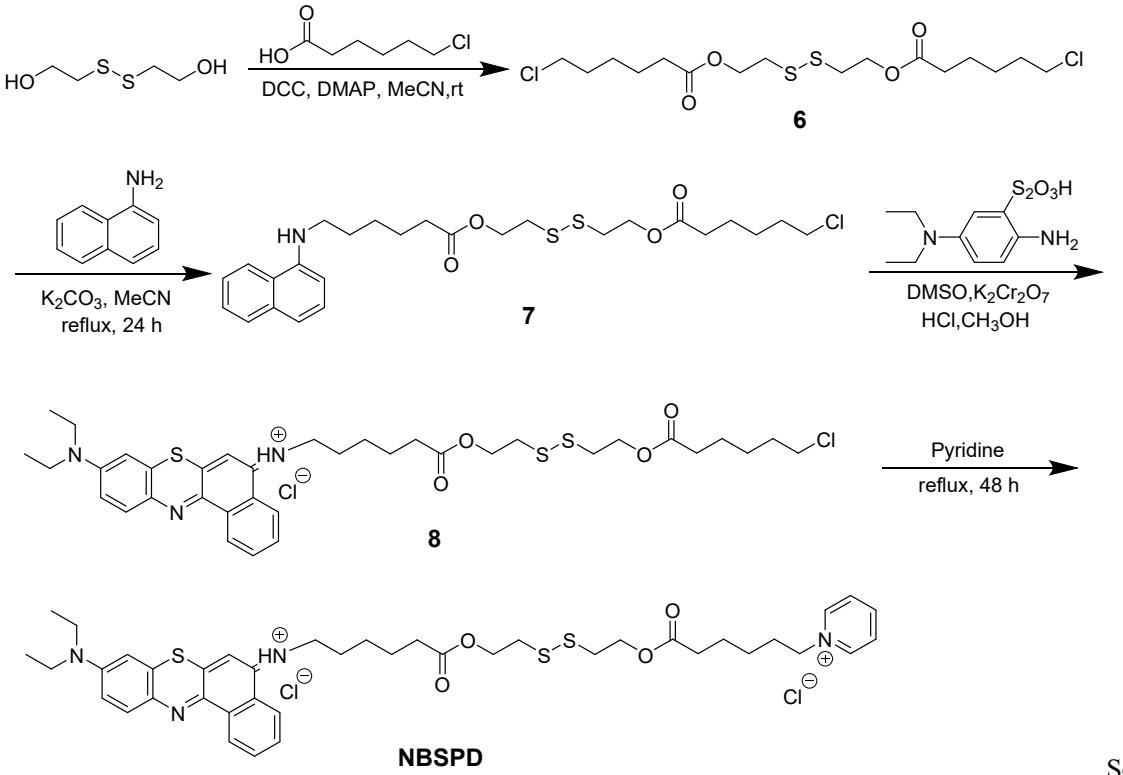

Scheme S2

Synthetic route of NBSPD.

Compounds 6, 7, 8, and NBSPD were synthesized according to our previous method.[3]

The ^{1}H NMR and ^{13}C NMR spectrums of compound 6 were shown in Fig. S9-10. ^{1}H NMR (500 MHz, $CDCl_3$, 298 K) δ (ppm): 4.33 (t, J = 6.55 Hz, 4H), 3.40 (t, J = 7.75 Hz, 4H), 2.92 (t, J = 6.55 Hz, 4H), 2.34 (t, J = 7.45 Hz, 4H), 1.90-1.84 (m, 4H), 1.69-1.62 (m, 4H), 1.51-1.44 (m, 4H). ^{13}C NMR (125 MHz, $CDCl_3$, 298 K) δ (ppm): 173.3, 62.2, 37.4, 34.0, 33.6, 32.5, 27.7, 24.1.

The ^{1}H NMR and ^{13}C NMR spectrums of compound 7 were shown in Fig. S11-12. ^{1}H NMR (500 MHz, $CDCl_3$, 298 K) δ (ppm): 7.81-7.77 (m, 2H), 7.45-7.40 (m, 2H), 7.34 (t, J = 15.7 Hz, 1H), 7.21 (d, J = 8.2 Hz, 1H), 6.59 (d, J = 7.5 Hz, 1H), 4.32 (q, J = 6.4 Hz, 4H), 3.38 (t, J = 6.8 Hz, 2H), 3.27 (t, J = 7.1 Hz, 2H), 2.90 (td, J = 6.6, 3.0 Hz, 4H), 2.37 (t, J = 7.4 Hz, 2H), 2.32 (t, J = 7.4 Hz, 2H), 1.85-1.82 (m, 2H), 1.79-1.76 (m, 2H), 1.74-1.71 (m, 2H), 1.66-1.60 (m, 2H), 1.55-1.49 (m, 2H), 1.47-1.43 (m, 2H). ^{13}C NMR (125 MHz, $CDCl_3$, 298 K) δ (ppm): 173.4, 173.2, 143.5, 134.3, 128.7, 126.7, 125.7, 124.6, 123.3, 119.9, 117.1, 104.2, 62.1, 44.0, 37.3, 37.2, 34.1, 33.9, 33.6, 32.4, 29.0, 27.6, 26.8, 24.7, 24.0.

The ^{1}H NMR and ^{13}C NMR spectrums of compound 8 were shown in Fig. S13-14. ^{1}H NMR (500 MHz, $CDCl_3$, 298 K) δ (ppm): 11.22 (s, 1H), 9.12 (d, J = 7.6 Hz, 1H), 8.73-8.71 (m, 1H), 7.74 (d, J = 9.4 Hz, 1H), 7.63-7.59 (m, 2H), 7.01 (dd, J = 9.4, 2.5 Hz, 1H), 6.8 (s, 1H), 6.75 (d, J = 2.5

Hz,1H), 4.29-4.26 (m, 4H), 3.72 (t, J = 7.3 Hz, 2H), 3.58 (q, J = 7.1 Hz, 4H), 3.49 (t, J = 6.6 Hz, 2H), 2.87 (t, J = 6.5 Hz, 4H), 2.34-2.28 (m, 4H), 1.90-1.84 (m, 2H), 1.76-1.57 (m, 6H), 1.53-1.47 (m, 2H), 1.45-1.39 (m, 2H), 1.30 (t, J = 7.1 Hz, 6H). ^{13}C NMR (125 MHz, $CDCl_3$, 298 K) δ (ppm): 173.4, 173.2, 154.0, 150.4, 139.7, 136.8, 135.3, 133.3, 131.9, 131.1, 130.1, 125.8, 125.2, 124.8, 116.0, 104.6, 102.7, 62.2, 62.1, 45.8, 44.9, 44.4, 37.3, 37.2, 33.96, 33.2, 28.9, 26.6, 26.4, 24.6, 24.2, 12.9.

The ^{1}H NMR and ^{13}C NMR spectrums of compound NBSPD were shown in Fig. S15-16. ^{1}H NMR (500 MHz, DMSO-d_6, 298.15 K) δ (ppm): 10.85 (s, 1H), 9.22 (m, 2H), 8.96 (d, J = 7.2 Hz, 1H), 8.88 (d, J = 7.4 Hz, 1H), 8.61 (t, J = 7.1Hz, 1H), 8.17 (s, 2H), 7.87 (s, 2H), 7.77 (t, J = 7.4 Hz, 1H), 7.51(s, 1H), 7.32 (s, 1H), 4.66 (t, J = 7.2 Hz, 2H), 4.26-4.17 (m, 4H), 3.7 (s, 2H), 3.66-3.59 (m, 4H), 2.95-2.91 (m, 4H), 2.35-2.27 (m, 4H), 1.95-1.87 (m, 2H), 1.80-1.73 (m, 2H),1.65-1.49 (m, 4H), 1.47-1.39 (m, 2H),1.30-1.18 (m, 8H). ^{13}C NMR (125 MHz, DMSO-d_6, 298.15 K) δ (ppm): 172.7, 172.5, 153.1, 150.6, 145.5, 144.8, 136.6, 133.8, 133.1, 131.7, 131.1, 129.4, 128.0, 124.5, 124.4, 120.0, 116.9, 105.3, 103.4, 99.5, 61.7, 61.6, 60.3, 59.4, 45.2, 45.0, 43.7, 41.0, 36.6, 36.4, 33.3, 33.0, 30.4, 28.1, 25.8, 24.7, 24.1, 23.7, 12.6.

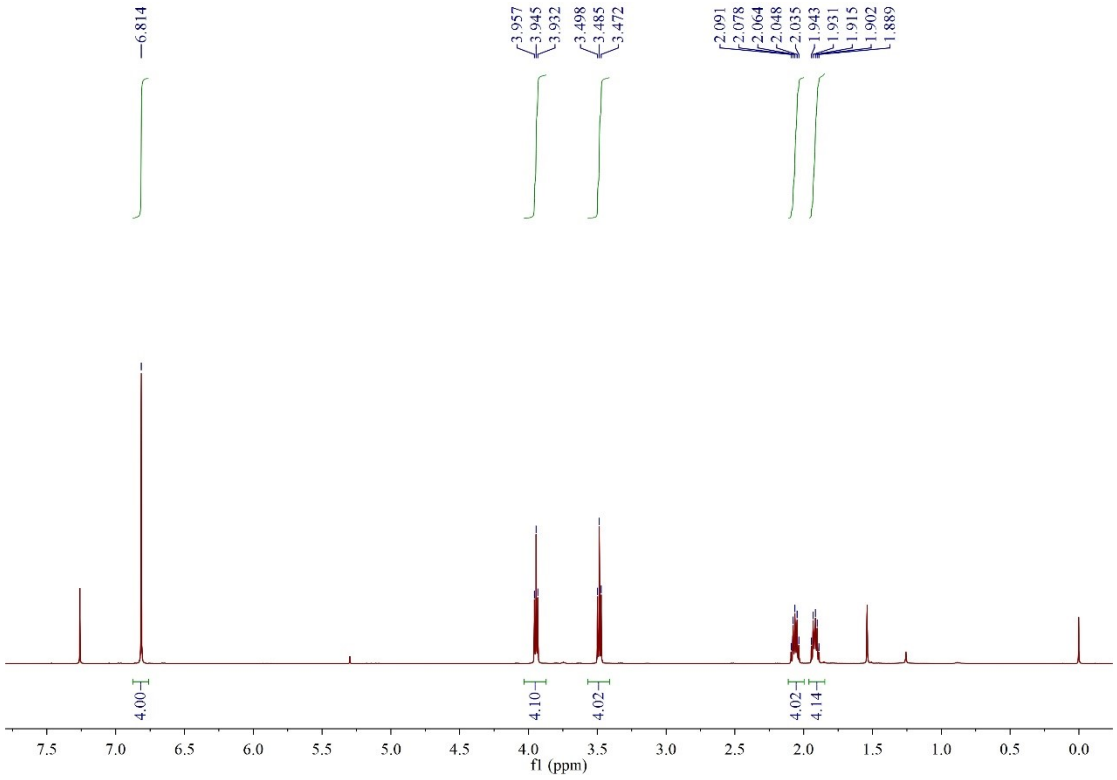

Fig. S1 ^{1}H NMR (500 MHz, $CDCl_3$, 298.15 K) spectrum of compound 1.

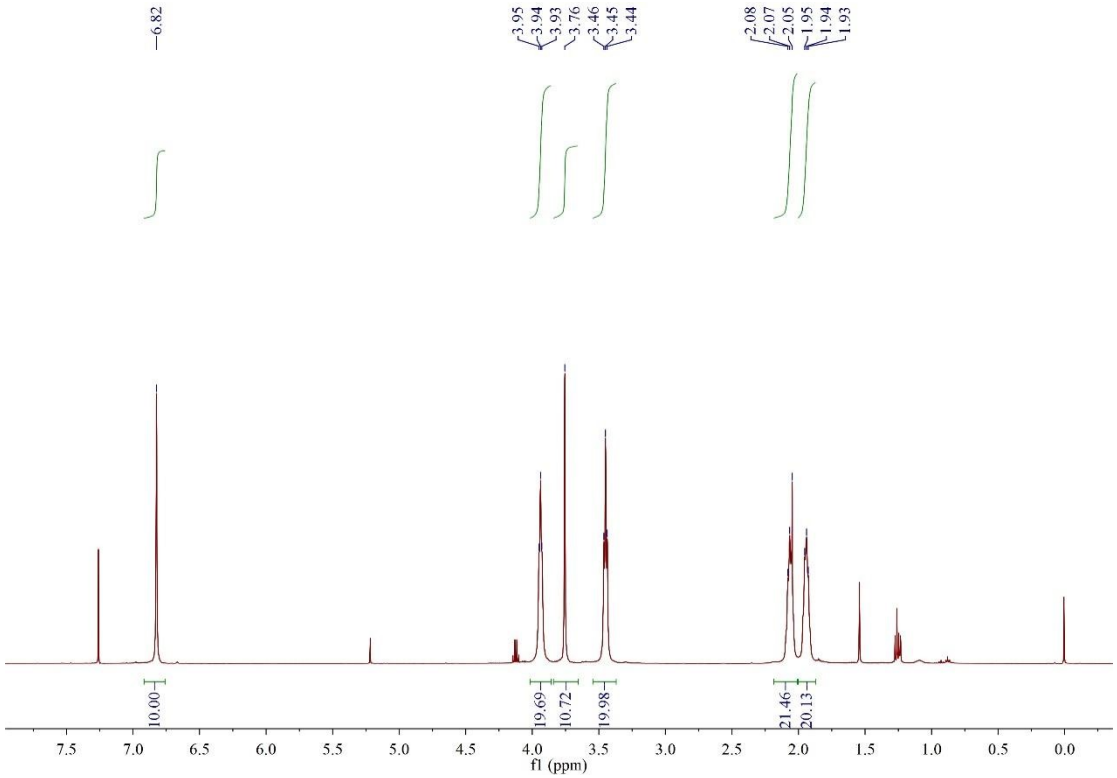

Fig. S2 ^{1}H NMR (500 MHz, $CDCl_3$, 298.15 K) spectrum of compound 2.

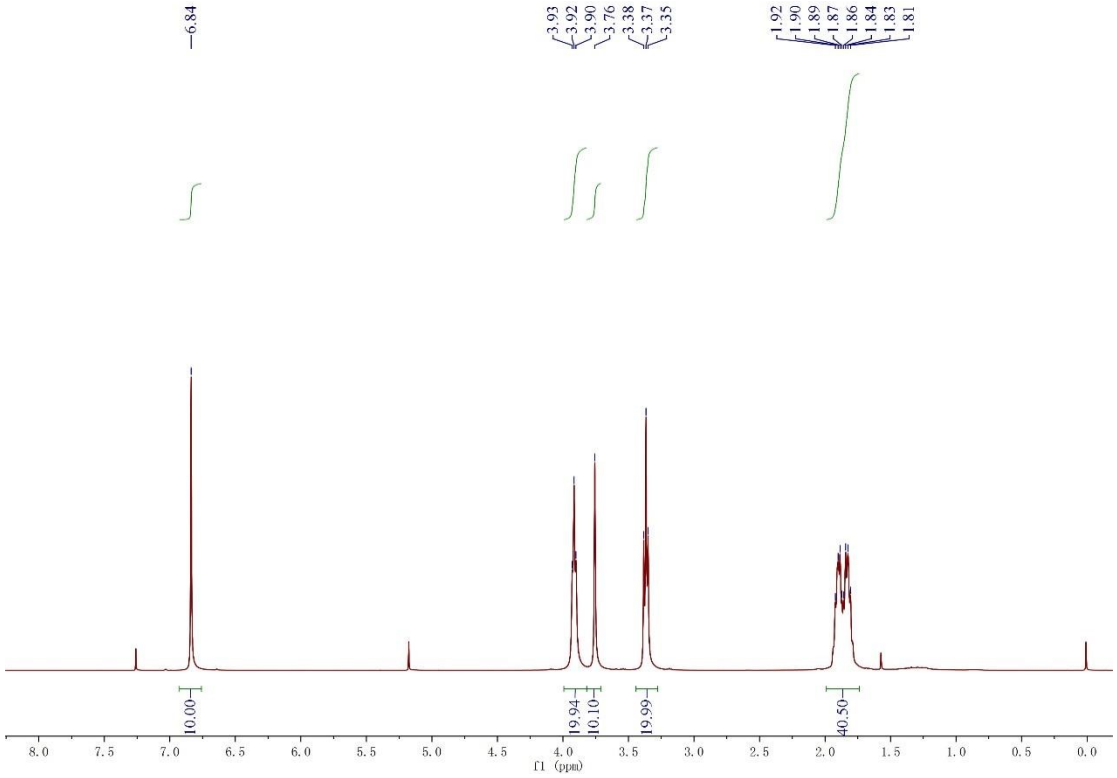

Fig. S3 ^{1}H NMR (500 MHz, $CDCl_3$, 298.15 K) spectrum of compound 3.

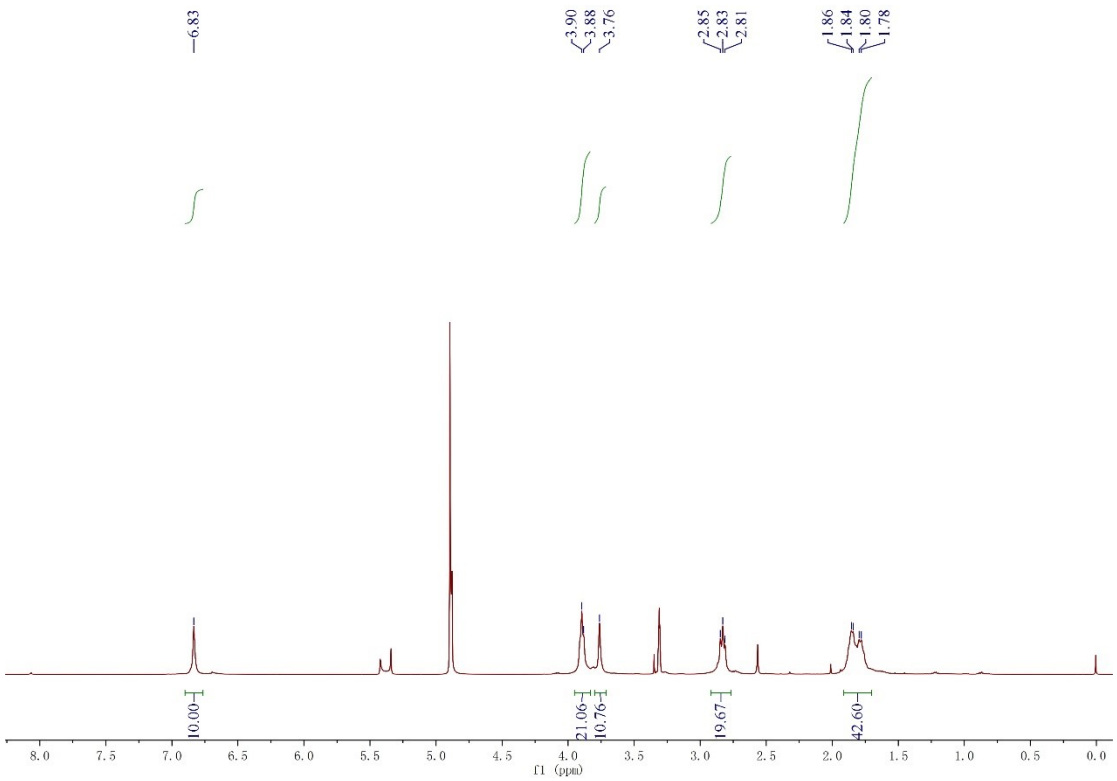

Fig. S4 ^{1}H NMR (400 MHz, MeOH-d_4, 298.15 K) spectrum of compound 4.

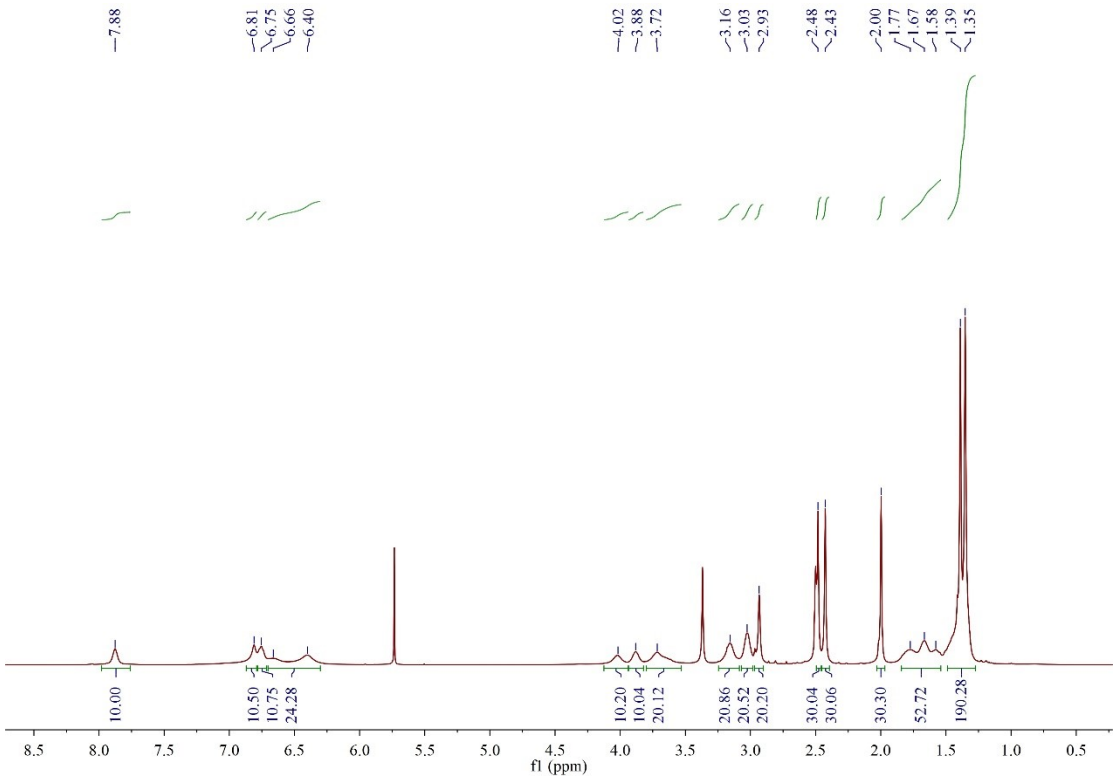

Figure S5 ^{1}H NMR (400 MHz, DMSO-d_6, 298.15 K) spectrum of compound 5.

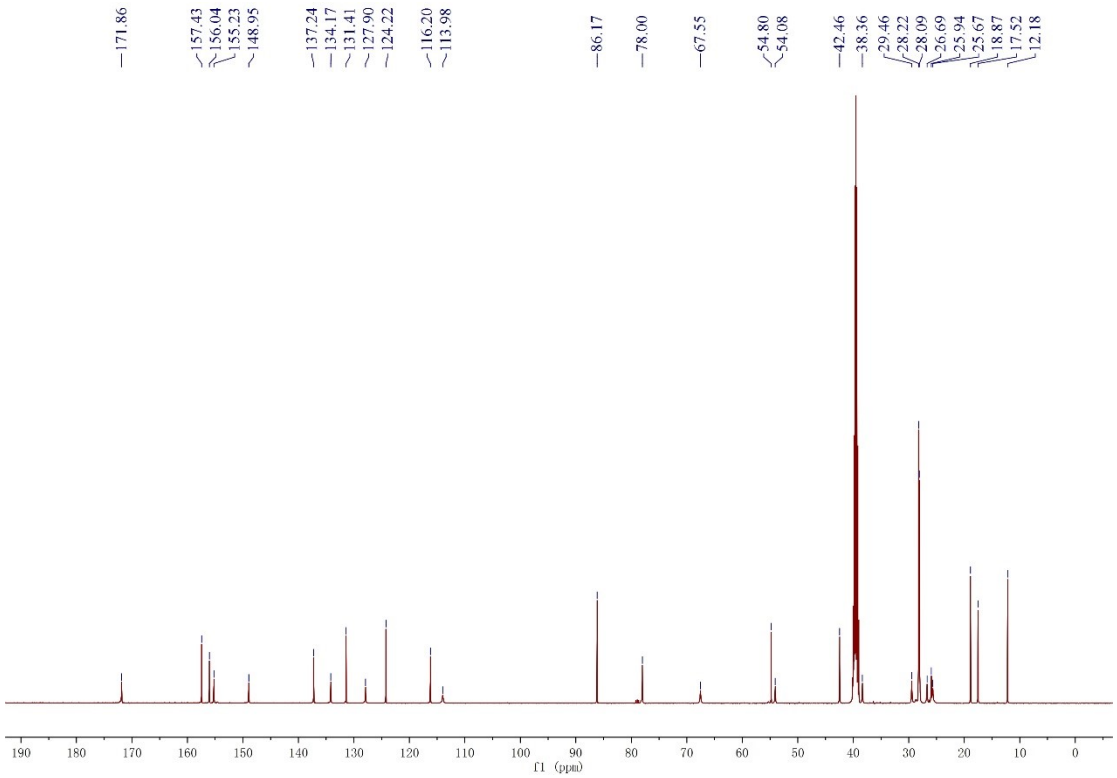

Figure S6 ^{13}C NMR (125 MHz, DMSO-d_6, 298.15 K) spectrum of compound 5.

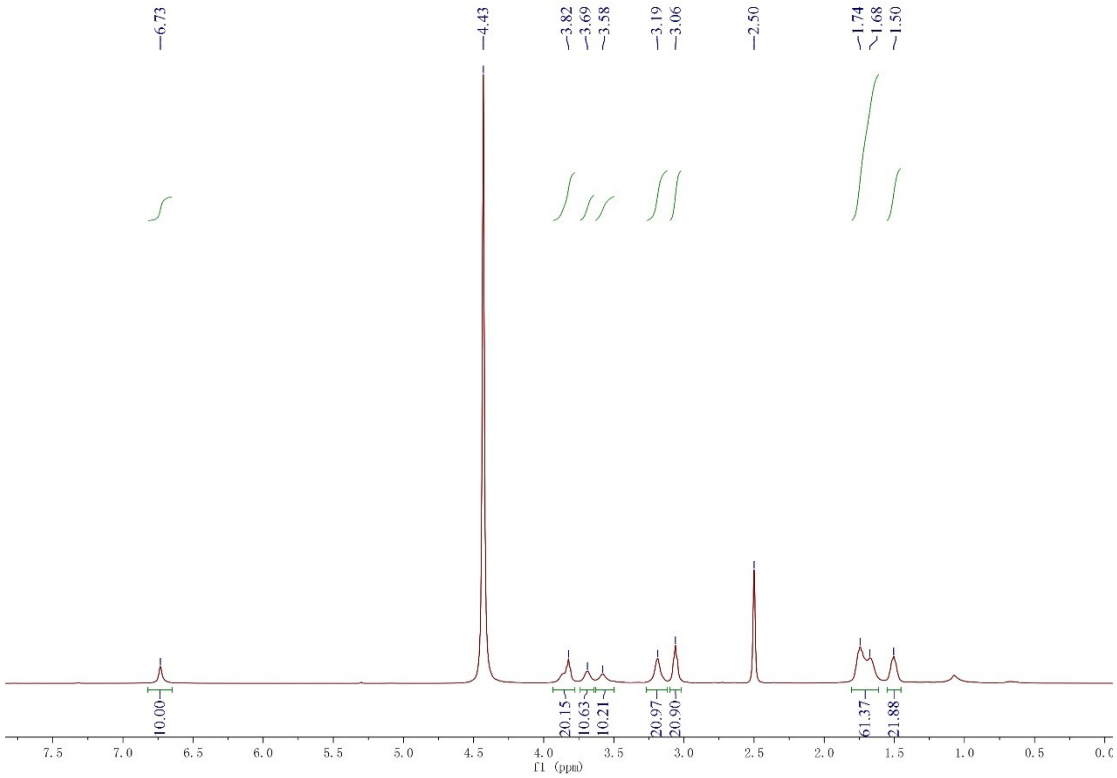

Fig. S7 ^{1}H NMR (400 MHz, D_2O/DMSO-d_6 = 1/1, 298.15 K) spectrum of compound LAP5.

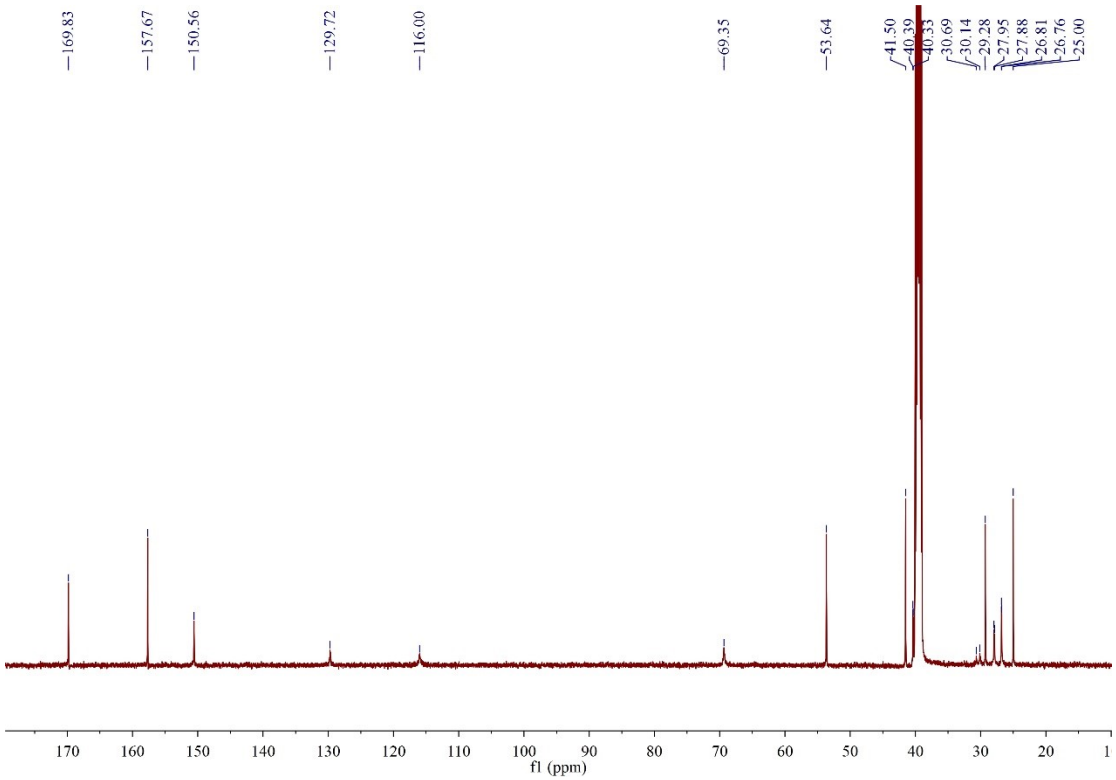

Fig. S8 ^{13}C NMR (125 MHz, D_2O/DMSO-d_6 = 1/1, 298.15 K) spectrum of compound LAP5.

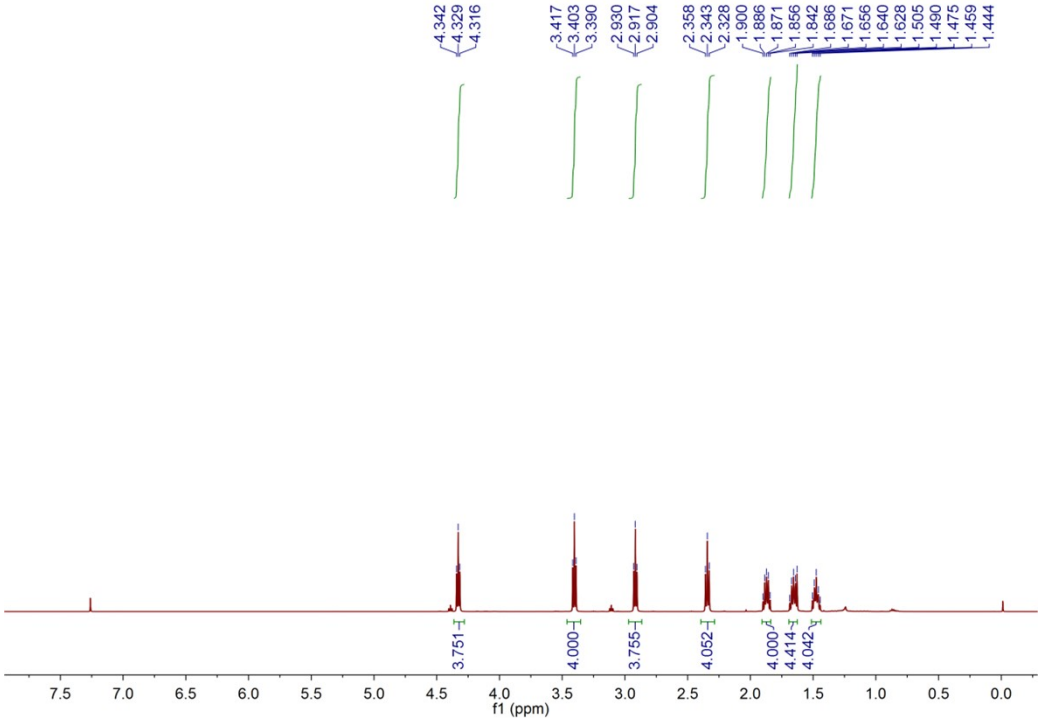

Fig. S9 ^{1}H NMR (500 MHz, $CDCl_3$, 298.15 K) spectrum of compound 6.

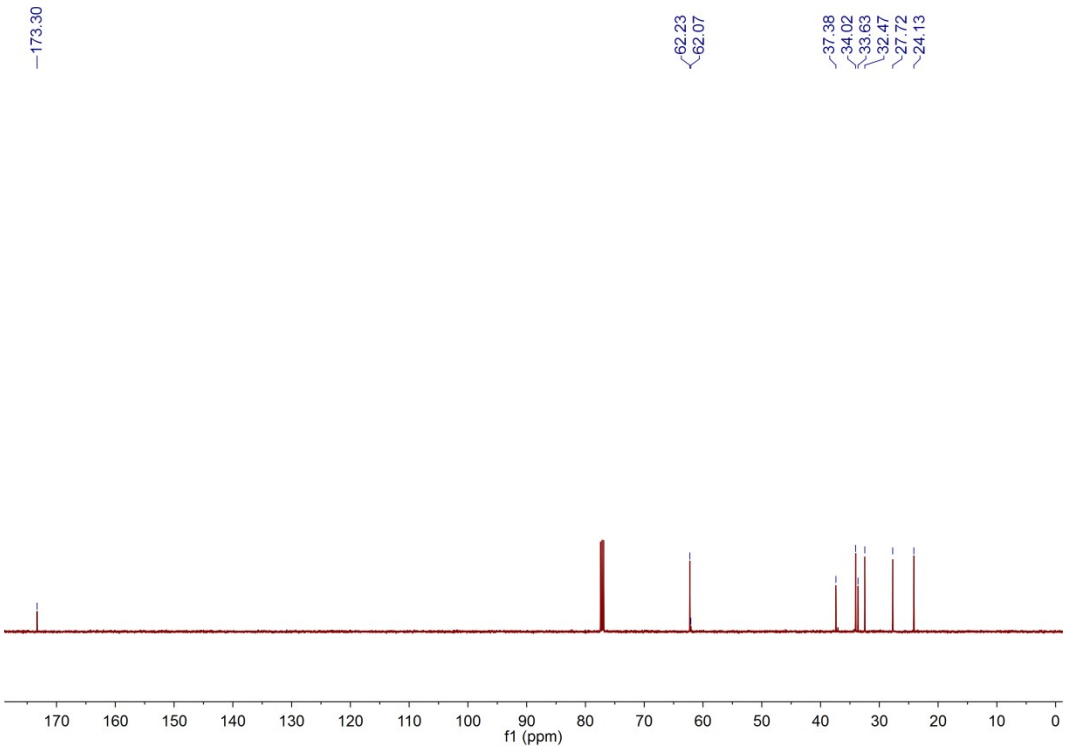

Fig. S10 ^{13}C NMR (125 MHz, $CDCl_3$, 298 K) spectrum of Compound 6.

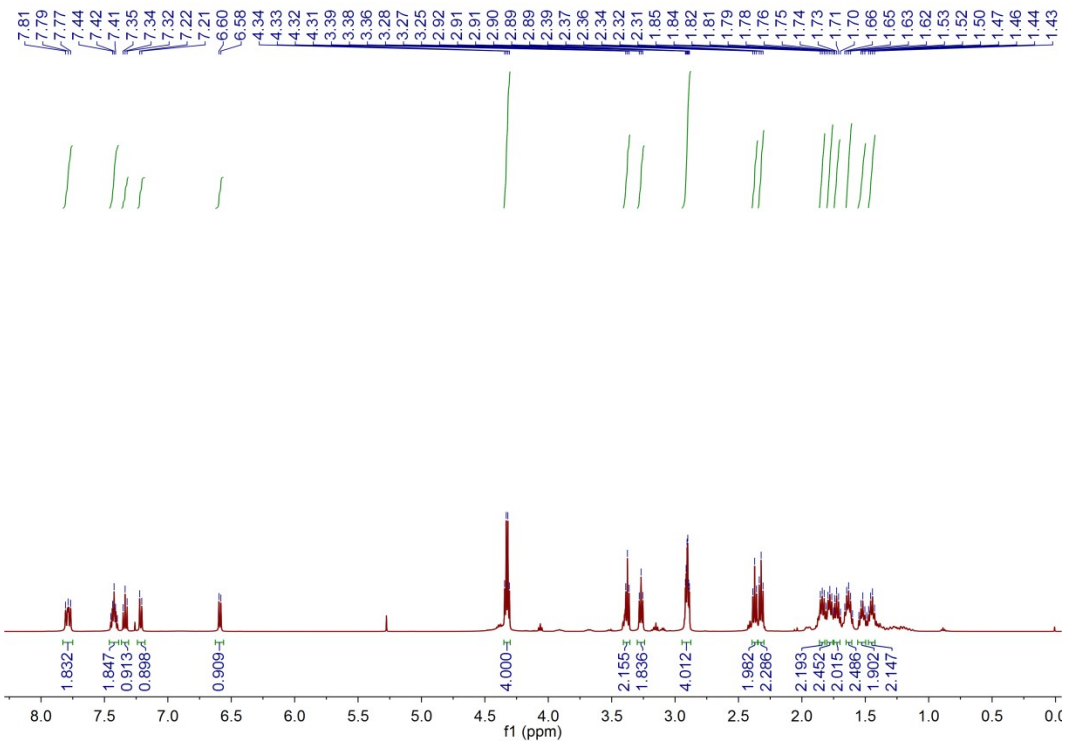

Fig. S11 ^{1}H NMR (500 MHz, $CDCl_3$, 298.15 K) spectrum of compound 7.

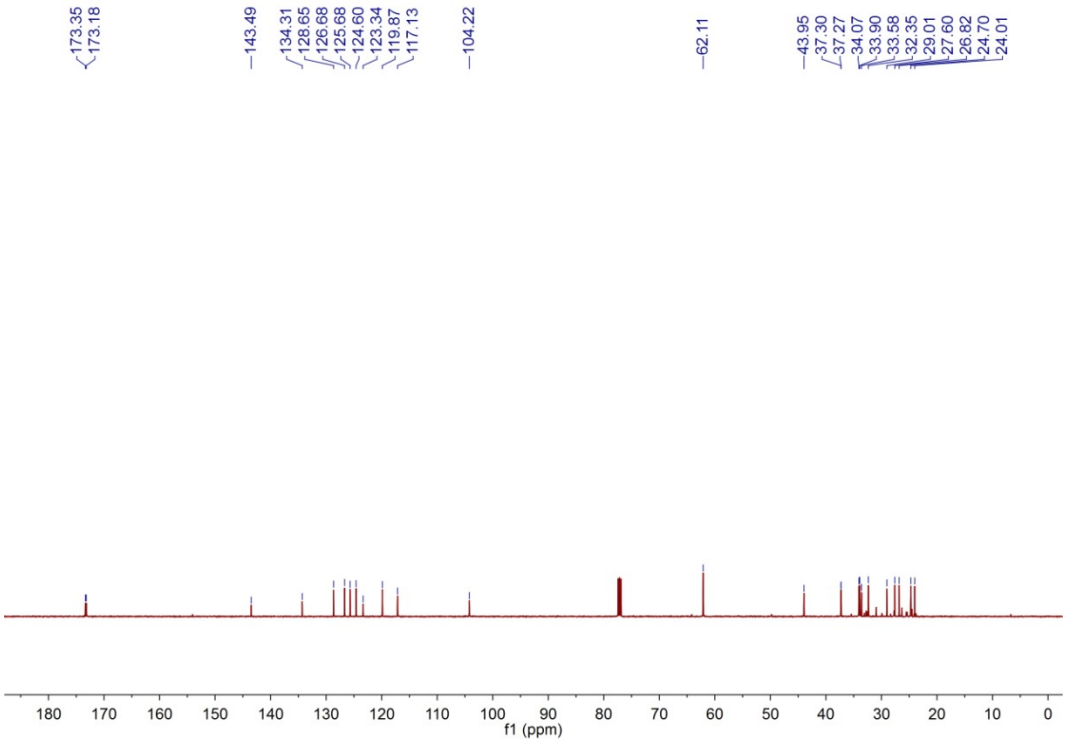

Fig. S12 ^{13}C NMR (125 MHz, $CDCl_3$, 298 K) spectrum of Compound 7.

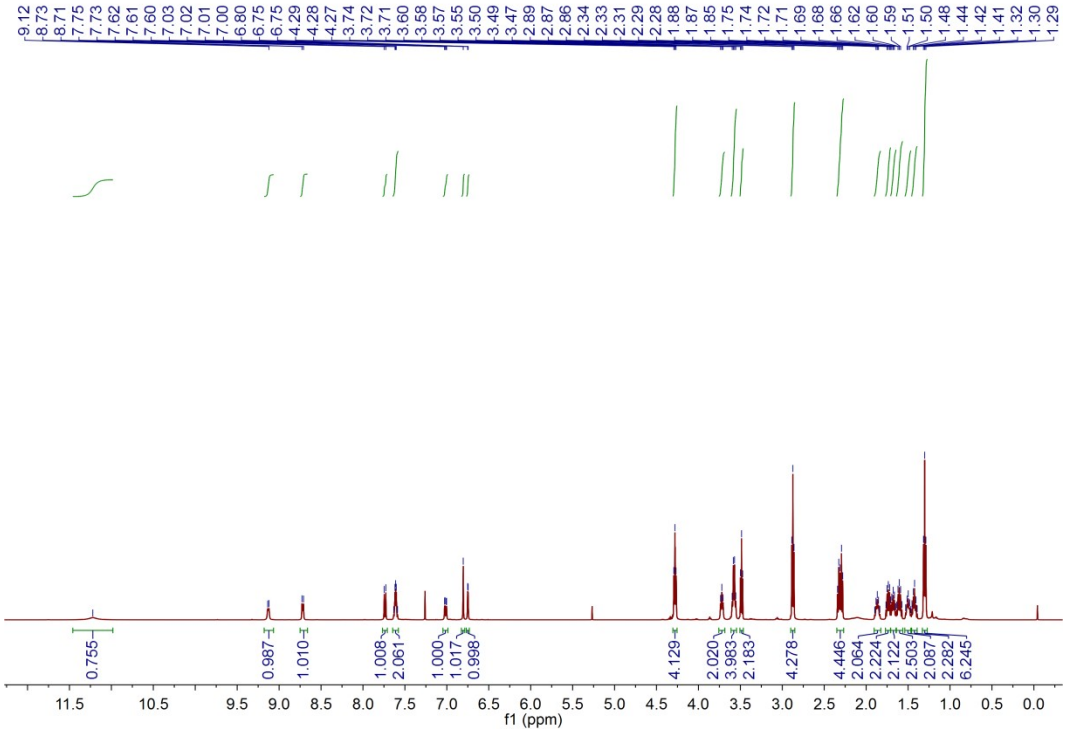

Fig. S13 ^{1}H NMR (500 MHz, $CDCl_3$, 298.15 K) spectrum of compound 8.

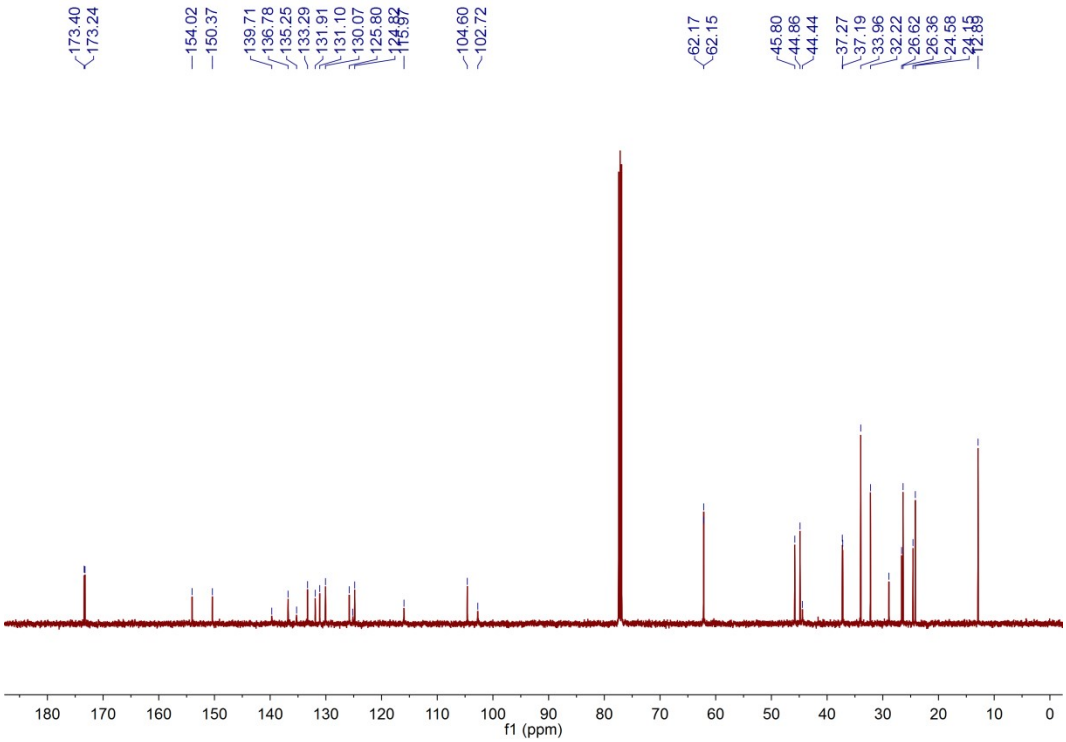

Fig. S14 ^{13}C NMR (125 MHz, $CDCl_3$, 298 K) spectrum of Compound 8.

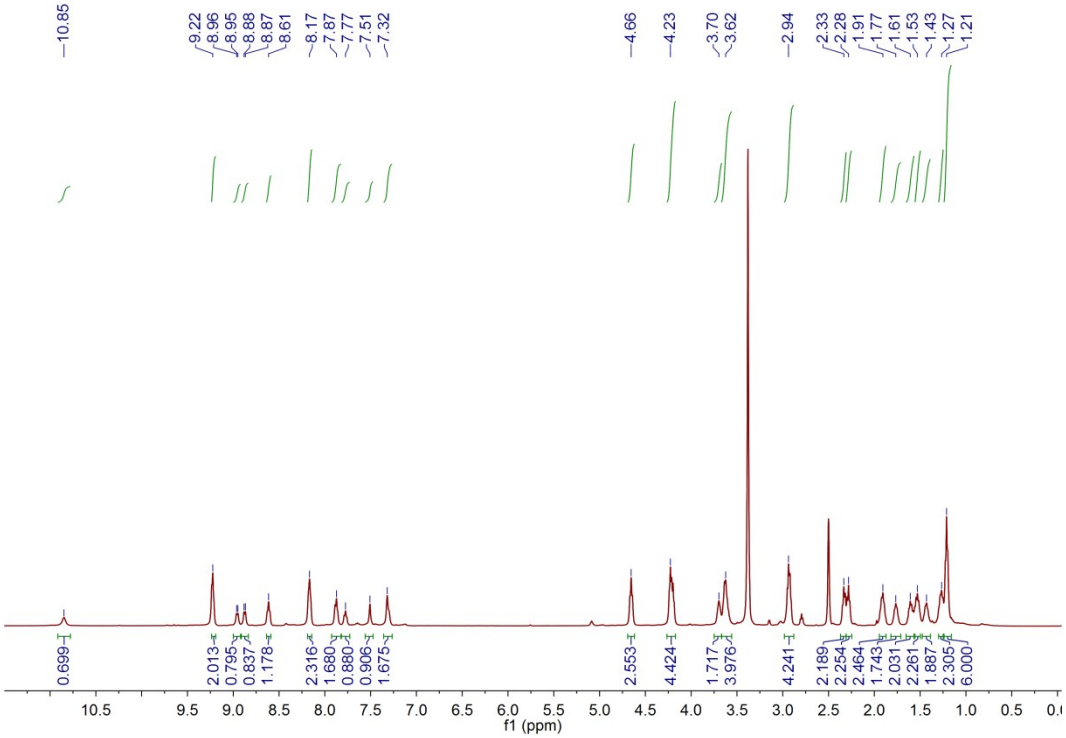

Fig. S15 ^{1}H NMR (500 MHz, DMSO-d_6, 298.15 K) spectrum of compound NBSPD.

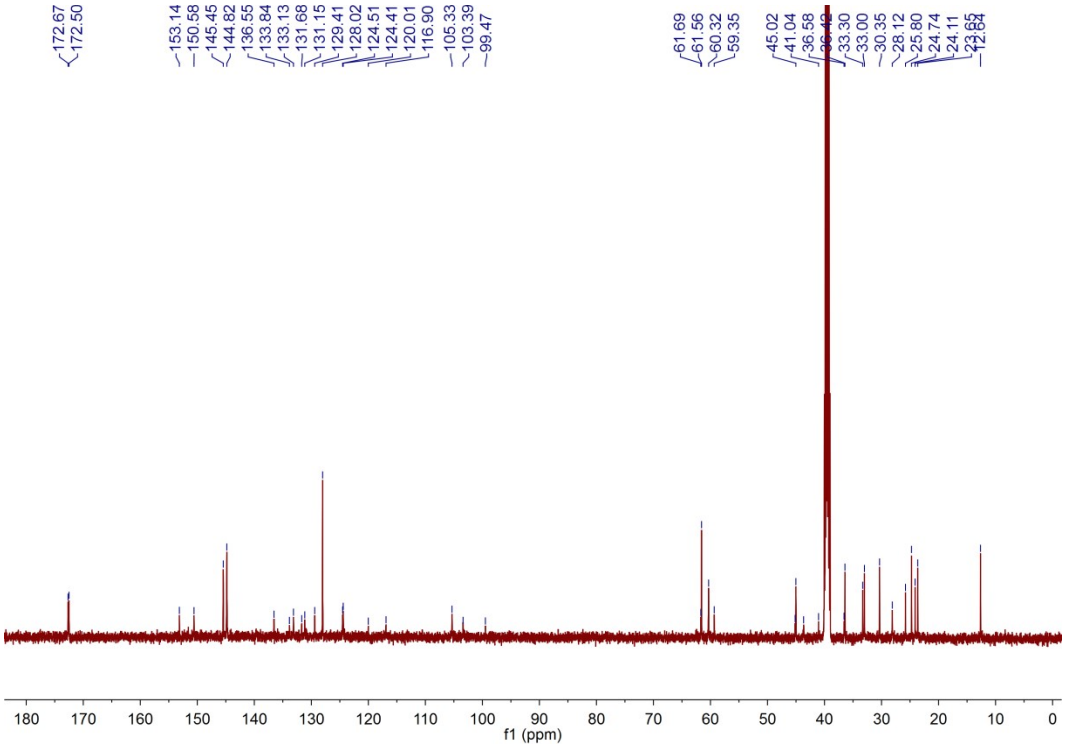

Fig. S16 ^{13}C NMR (125 MHz, DMSO-d_6, 298.15 K) spectrum of compound NBSPD.

4. Raw ITC data of LAP5 with NBSPD in water

The binding constant between LAP5 and NBSPD was performed using a thermostated and fully computer operated Nano-ITC SV calorimeter purchased from TA-Waters LLC. The microcalorimetric titrations were performed in D.I. water at atmospheric pressure. Each solution was degassed and thermostated before titration.

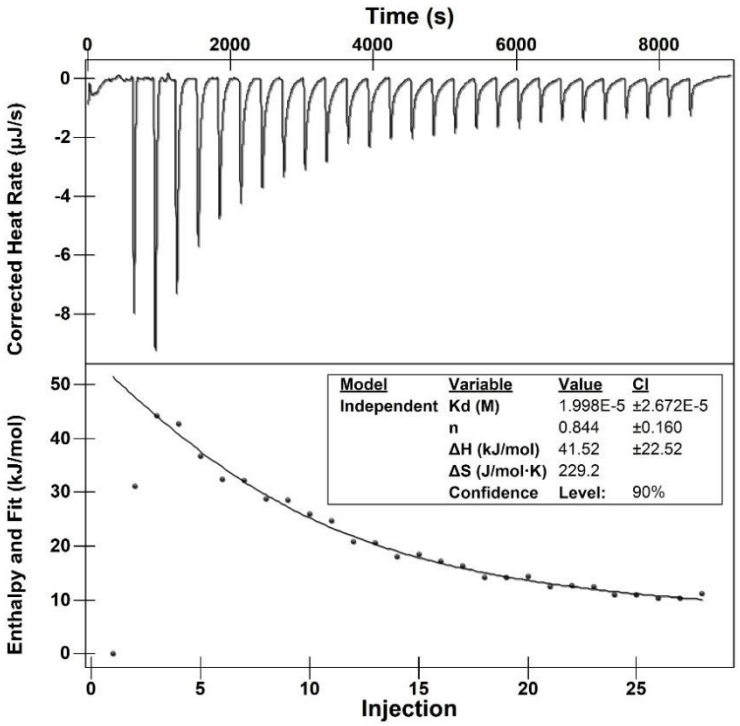

Fig. S17 ITC Microcalorimetric titration of LAP5 and NBSPD in D.I. water at 298.15 K. (TOP) Raw ITC data for 28 sequential injections (3.54 µL per injection) of a LAP5 solution (2.00 mM) into a NBSPD solution (0.10 mM). (Bottom) Net reaction heat obtained from the integration of the calorimetric traces.

5. Job's Plot for LAP5⊃NBSPD

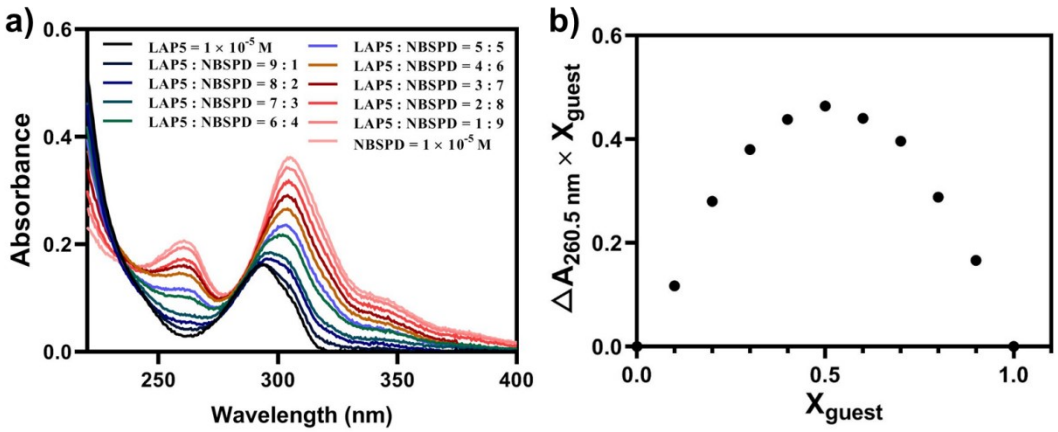

Fig. S18 (a) Absorption intensity of the mixture of LAP5 and NBSPD in water at different molar ratio while [LAP5] + [NBSPD] = 1 ×10^{-5} M; (b) Job's Plot showing 1:1 stoichiometry of the complex between LAP5 and NBSPD by plotting the difference fluorescence intensity at 260.5 nm.

6. Tyndall effect and size distribution statistics data

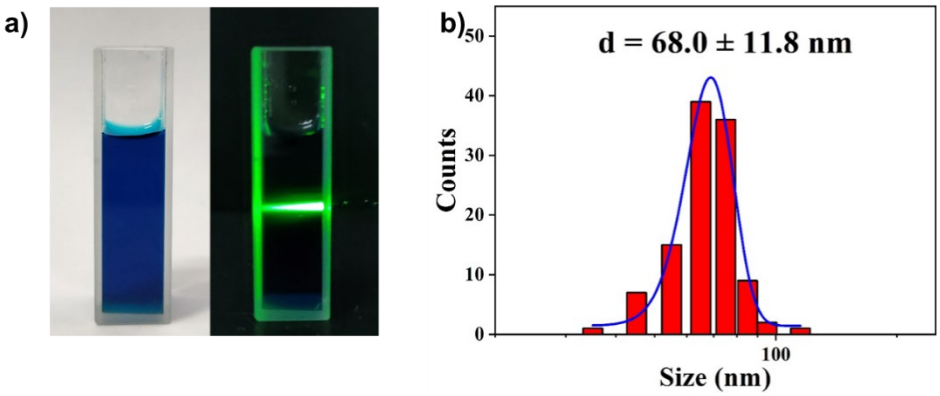

Fig. S19 (a) The obvious Tyndall effect of LAP5⊃NBSPD NPs; (b) Size distribution statistics data of LAP5⊃NBSPD NPs in SEM results.

7. Analysis of LAP5⊃NBSPD NPs cellular internalization pathways

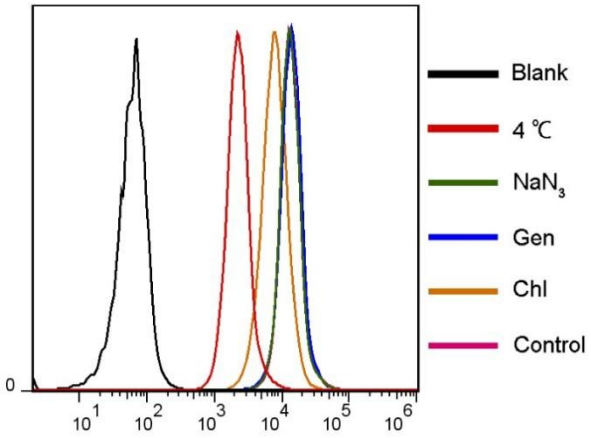

Fig. S20 Internalisation of NBS on HepG2 cells after 2 h incubation with 1.28 μM LAP5⊃NBSPD NPs under different inhibitory conditions as measured by flow cytometry.

8. Co-localization of NBS with lysosomes

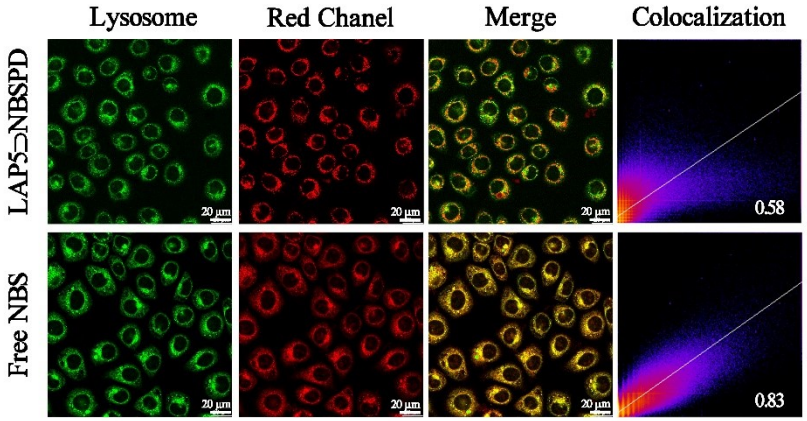

Fig. S21 Co-localization of NBS with lysosomes were detected *via* CLSM after HepG2 was treated with

LAP5⊃NBSPD NPs and Free NBS for 1 h. The scale bar is 20 μm.

9. In vitro ROS detection results

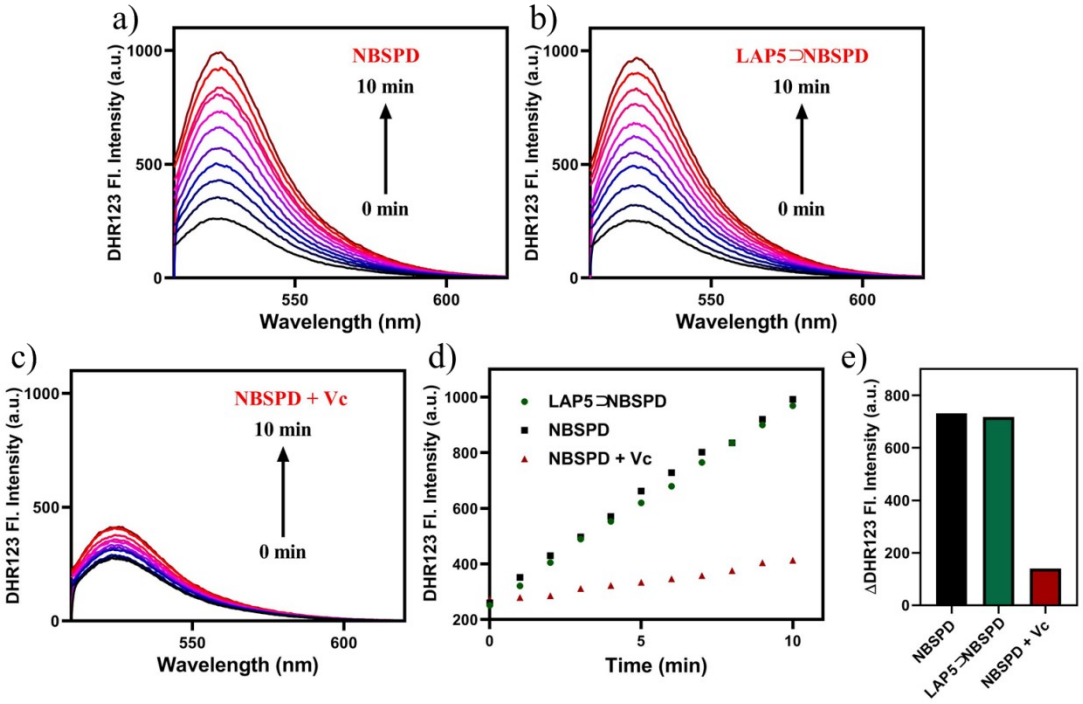

Fig. S22 $O_2^{-\bullet}$ production and characterization using DHR123 as fluorescence probe: Fluorescence spectra of DHR123 (10 μM) induced by (a) NBSPD (10 μM), b) LAP5⊃NBSPD (10 μM) and c) NBSPD (10 μM) + Vc (100 μM) after 630 nm light irradiation (20 mW/cm^2); (d-e) Fluorescence intensity of DHR123 at 525 nm after 660 nm irradiation for 10 min.

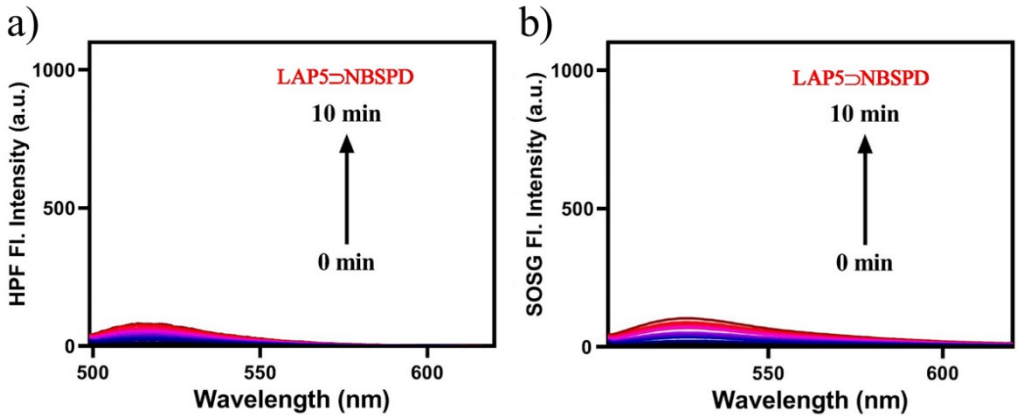

Fig. S23 Fluorescence curves of (a) HPF (10 μM) for OH• characterization and (b) SOSG (10 μM) for $^1O_2$ detection induced by LAP5⊃NBSPD (10 μM) after 660 nm light irradiation (20 mW/cm^2).

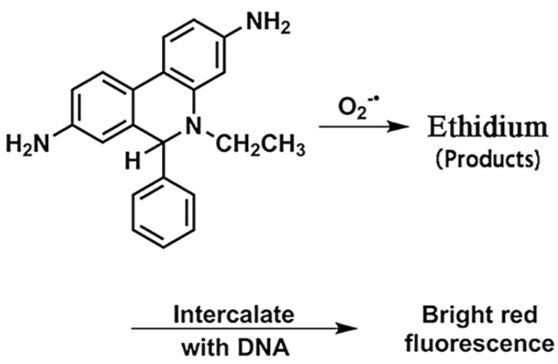

Fig. S24 Detection mechanism of DHE for $O_2^{-\bullet}$.

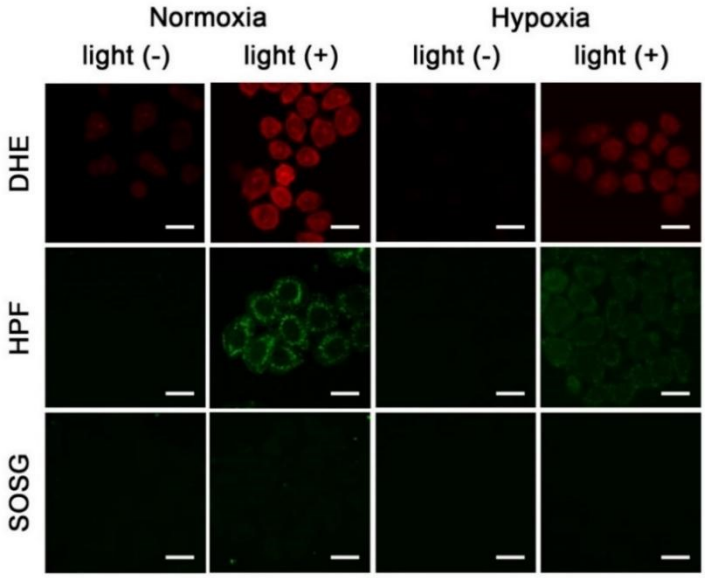

Fig. S25 ROS detection in HepG2 cells after 1 h incubation with 1.28 μM LAP5⊃NBSPD NPs and exposure to 660 nm light with 15 J/cm^2 under normoxia and hypoxia conditions using DHE, HPF, and SOSG as the $O_2^{-\bullet}$, OH•, and $^1O_2$ fluorescence indicator, respectively. The scale bar is 20 μm.

10. Cellular morphological damage results of LAP5⊃NBSPD NPs

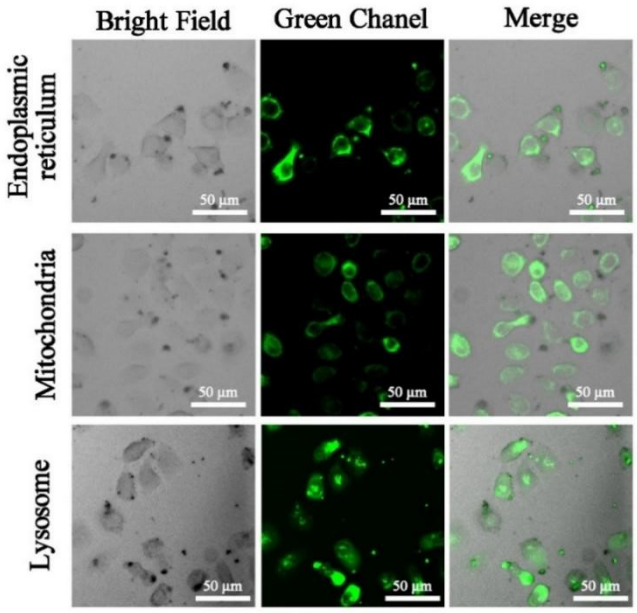

Fig. S26 Observation of morphological changes of organelles such as endoplasmic reticulum, mitochondria and lysosomes in HepG2 cells after 4 h incubation with 2.56 μM LAP5⊃NBSPD NPs by CLSM. The scale bar is 50 μm.

11. Cytotoxicity evaluation

HepG2 and HL7702 cells were cultured in RPMI 1640 medium containing 10% FBS, 1% penicillin/streptomycin (complete RPMI 1640 medium) in 5% CO_2 at 37 °C. Liquid paraffin covering method was used to simulate the tumor hypoxic environment. The relative cytotoxicity of LAP5, and LAP5⊃NBSPD NPs were evaluated *in vitro* by MTT assay, respectively. The cells were seeded in 96-well plates. Liquid paraffin was added on the surface of cell culture medium and incubated at 37 ℃ under 5% CO_2 for 24 h to obtain hypoxic state cells. The dark toxicity and phototoxicity of LAP5⊃NBSPD NPs was demonstrated on HepG2 and HL7702 cells for 24 h. Subsequently, cells were washed and the fresh medium containing MTT (0.5 mg/mL) was added into each plate. The cells were incubated for another 4 h. After that, the medium containing MTT was removed and dimethyl sulfoxide (100 μL) was added to each well to dissolve the formazan crystals. Finally, the plate was gently shaken for 10 min and the absorbance at 490 nm was recorded with a microplate reader.

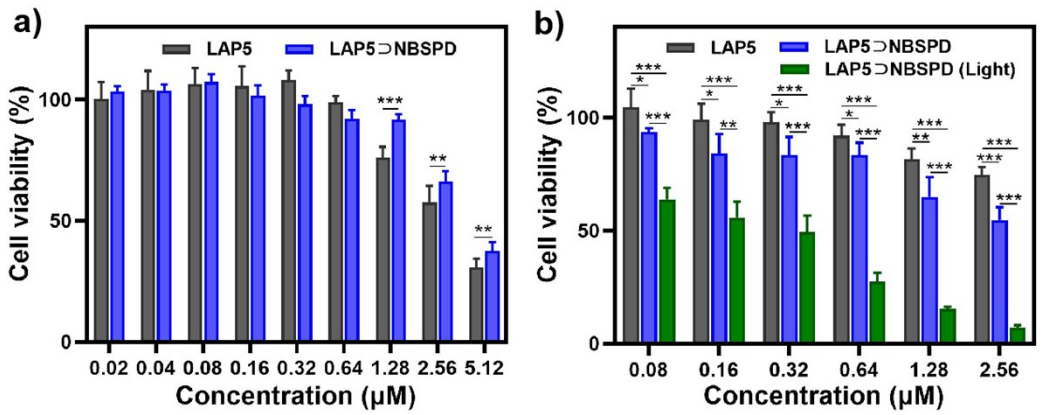

Fig. S27 (a) The dark toxicity of LAP5 and LAP5⊃NBSPD NPs on HL7702 cells without light irradiation for 24 h; (b) The cytotoxicity results of free LAP5 and LAP5⊃NBSPD NPs on HepG2 cells under hypoxia conditions for 24 h after 660 nm light irradiation (15 J/cm^2). (n = 6, $^*P < 0.05$, $^{**}P < 0.01$, $^{***}P < 0.001$)

12. References

1 Y. Chang, K. Yang, P. Wei, S. Huang, Y. Pei, W. Zhao and Z. Pei, *Angew. Chem. Int. Ed.*, 2014, **53**, 13126-13130.

2 K. Yang, Y. Chang, J. Wen, Y. Lu, Y. Pei, S. Cao, F. Wang and Z. Pei, *Chem. Mat.*, 2016, **28**, 1990-1993.

3 S. Chao, Z. Shen, Y. Pei, Y. Lv, X. Chen, J. Ren, K. Yang and Z. Pei, *Chem. Commun.*, 2021, **57**, 7625-7628.